Ocean Sci. Discuss., 7, 1405–1437, 2010
www.ocean-sci-discuss.net/7/1405/2010/
doi:10.5194/osd-7-1405-2010

Ocean Science Discussions

Influence of cross-shelf water transport on nutrients and phytoplankton in the East China Sea: a model study

L. Zhao[1] **and X. Guo**[2]

[1]Physical Oceanography Laboratory, Ocean University of China, 238 Songling Road, Qingdao, 266100, China
[2]Center for Marine Environmental Studies, Ehime University, 2-5 Bunkyo-Cho, Matsuyama, 790-8577, Japan

Received: 12 June 2010 – Accepted: 13 July 2010 – Published: 26 July 2010

Correspondence to: X. Guo (guoxinyu@dpc.ehime-u.ac.jp)

Published by Copernicus Publications on behalf of the European Geosciences Union.

Abstract

A three dimensional coupled biophysical model was used to examine the supply of oceanic nutrients to the shelf of the East China Sea (ECS) and its role in primary production over the shelf. The model consisted of two modules: the hydrodynamic module was based on a nested model with a horizontal resolution of 1/18 degree, whereas the biological module was a low trophic level ecosystem model including two types of phytoplankton, three elements of nutrients, and biogenic organic material. Model results suggested that seasonal variation in chlorophyll-*a* had a strong regional dependence over the shelf of the ECS. The area with high chlorophyll-*a* appears firstly at the outer shelf in winter, and gradually migrates toward the inner shelf (offshore region of Changjiang estuary) from spring to summer. Vertically, chlorophyll-*a* was generally homogenous from the coastal zone to the inner shelf. In the middle and outer shelves, high chlorophyll-*a* appeared in the surface in spring but moved to the subsurface from summer to early autumn. The annual averaged onshore flux across the shelf break was estimated to be 1.53 Sv for volume, 9.4 kmol s^{-1} for DIN, 0.7 kmol s^{-1} for DIP, and 18.2 kmol s^{-1} for silicate, which are supplied mainly from the northeast of Taiwan and southwest of Kyushu. From calculations that artificially increased the concentration of nutrients in the Kuroshio water, the additional oceanic nutrients were distributed in the bottom layer from the shelf break to the region offshore of Changjiang estuary from spring to summer, and appeared in the surface layer from autumn to winter. The contribution of oceanic nutrients to primary production over the shelf was found not only in the surface layer (mainly at the outer shelf and shelf break in winter and in the region offshore of Changjiang estuary in summer) but also in the subsurface layer over the shelf from spring to autumn.

1 Introduction

In addition to the terrestrial input of nutrients, marginal seas also receive nutrients from the open ocean (hereafter referred to oceanic nutrients) through cross-shelf water exchange. From a timescale of several decades, terrestrial inputs are affected by both anthropogenic activities and climate change, with oceanic nutrients mainly driven by climate change. Quantifying the oceanic nutrient flux and evaluating its role in driving primary production in marginal seas therefore addresses two key issues in understanding potential influences of climate change on these economically and ecologically important ecosystems.

The East China Sea (ECS) is one of the major marginal seas of the northwestern Pacific (Fig. 1). Many rivers including the Changjiang River (Yangtze River) represent a substantial input of freshwater and nutrients into the adjacent sea (Zhang, 1996). On the other hand, the ECS also receives water and associated nutrients from the South China Sea through the Taiwan Strait, in which its volume transport is greater than river discharge into the ECS by as much as two orders of magnitude (Isobe, 2008). The ECS has a long shelf break (see 200 m-isobath in Fig. 1), by which onshore volume transport across the shelf break has been reported to be within the same order as that through the Taiwan Strait (Guo et al., 2006; Isobe, 2008).

There are strong seasonal variations in the spatial distribution of nutrients in the ECS (Chen, 2009). The concentration of surface nutrients in the ECS is high in winter, depletes in spring and summer, and reverts smoothly in autumn to the concentration in winter (Wang, et al., 2003; Chen, 2009). Such seasonal variations are tightly coupled to biological processes such as phytoplankton blooms in spring through summer and the remineralization of detritus in autumn as well as on the physical processes such as summer stratification and winter mixing. In addition, seasonal changes in inputs of terrestrial nutrients from rivers and of oceanic nutrient from the Taiwan Strait and the shelf break are also important to the concentration of nutrients in the ECS.

Using a box model, Chen and Wang (1999) calculated the annual nutrient budget over the shelf of the ECS and suggested a more important role of Kuroshio subsurface water in supplying nutrients onto the ECS shelf compared to rivers. Zhang et al. (2007b) revisited this calculation using data collected in summer and winter, respectively, and confirmed that nutrients supplied by Kuroshio subsurface water intrusion onto the shelf was important in both seasons, in particular for phosphate. These findings are supported by the distribution of passive tracer released only in the Kuroshio region east of Taiwan in a three dimensional numerical model (Guo et al., 2006).

Although oceanic nutrients have been shown to be important to the nutrient budget of the ECS (Chen and Wang, 1999; Zhang et al., 2007b), it is still unknown whether oceanic nutrients are readily utilized by phytoplankton over the shelf. If oceanic nutrients significantly contribute to primary production over the shelf of the ECS, we should clarify where and when primary production occurs, and to what extent is attributed to inputs from oceanic nutrients. Furthermore, we also need to address the physical processes that transport oceanic nutrients inside the Kuroshio subsurface water up to the euphotic zone in the shelf region. In this study, we applied a three dimensional numerical biophysical model to evaluate the role of oceanic nutrients in driving primary production in the ECS. The physical processes related to the transport of oceanic nutrients to the euphotic zone will be discussed by a companion paper in the near future.

Model configurations and calculation plans are described in Sect. 2. Then, we compared model results (nutrients and chlorophyll-*a*) with observations and examined the nutrient flux across the shelf break in the ECS by presenting its spatial distribution along the shelf break and its seasonal variations in Sect. 3. By changing the concentration of nutrients in the Kuroshio water, we reran the simulations and examined changes in concentrations of nutrients and chlorophyll-*a* over the shelf of the ECS, and in the onshore nutrient flux across shelf break in Sect. 4. Finally, we summarize this study in Sect. 5.

2 Model configuration and data sources

Our model consisted of two modules, a hydrodynamic module and a biological module. The hydrodynamic module provided physical parameters such as water temperature, velocities and diffusivity coefficients to the biological module that is online coupled to the hydrodynamic module, i.e., the two modules were run simultaneously.

The hydrodynamic module is based on the Princeton Ocean Model (Blumberg and Mellor, 1987; Mellor, 2003) and configured with a nesting method to obtain high horizontal resolution (1/18 degree) for the ECS, as described in details by Guo et al. (2003). In the vertical, 21 sigma levels were used. Differences from the previous version were the explicit inclusion of freshwater input from sea surface and rivers and the addition of tidal forcing (M_2, S_2, K_1 and O_1 tides) along the lateral boundary (Wang et al., 2008).

The biological module is based on the biological part of NORWECOM (Skogen and Søiland, 1998) and reconstructed for the ECS. The model components include three elements of nutrients (dissolved inorganic nitrogen, DIN; dissolved inorganic phosphorus, DIP; and silicate, SIL), two types of phytoplankton (diatoms, DIA; and flagellates, FLA), and two types of biogenic organic material (dead organic matter, DET; and biogenic silica, SIS). A schematic diagram showing relationships among these components is presented in Fig. 2.

The biological module treats the water column and benthic layer as two individual parts. Biological processes in the water column include photosynthesis, respiration and mortality of phytoplankton, remineralization of detritus and the shading effects of phytoplankton on underwater light. Because of the high turbidity in the ECS, concentrations of suspended particulate matter (SPM) from satellite-based data (Wang and Jiang, 2008) were included in the biological module to determine the extinction coefficient of photosynthatic active radiation that is affected by the concentrations of both SPM and chlorophyll-*a*. Processes in the benthic layer are remineralization of detritus, sediment burial and denitrification. Sedimentation and resuspension through the sediment-water interface and the atmospheric dry and wet deposition of nutrients

through the air-sea interface are included in the biological module. The equations for the biochemical processes follow those given by Skogen and Søiland (1998). Parameters used in the equations for biochemical processes were based on the values in the literature (Moll, 1998; Skogen and Moll, 2000; Wei et al., 2004), but were adjusted by trial and error.

The model domain covers the Bohai Sea, Yellow Sea and ECS with the open boundary along southern and eastern boundaries (Fig. 1). With the objective of reproducing seasonal variation, the hydrodynamic module was driven by monthly forcing such as river runoff, wind stress, heat flux, evaporation and precipitation rates, ocean and tidal currents, as described by Wang et al. (2008). The biological module was also prescribed the same monthly conditions to reproduce spatial distributions of nutrients and chlorophyll-*a* and their seasonal variations.

Calculation was started with an initial condition in winter and was spun up for two years; model results in the third year were analyzed. The initial and open boundary conditions for three elements of nutrients are from World Ocean Atlas 2005 (WOA2005) (Garcia et al., 2006a; 2006b) and Marine Atlas of Bohai Sea, Yellow Sea, East China Sea, Chemistry (Wang, 1991), and monthly SPM concentrations were from SeaWiFS-derived data (Wang and Jiang, 2008). Runoff from ten major rivers (Fig. 1) were from the Marine Atlas of Bohai Sea, Yellow Sea, East China Sea, Hydrology (Chen, 1992). The concentrations of nutrients in rivers and those for atmospheric dry and wet deposition of nutrients were obtained from published data (Zhang, 1996; Liu et al., 2009; Wan et al., 2002; Zhang et al., 2007a). Solar radiation was calculated by the model given by Dobson and Smith (1988) and cloud cover data was from NCEP/NCAR reanalysis (Kalnay et al., 1996). The validation data of nutrients and chlorophyll-*a* were from the Japan Meteorological Agency (JMA) monitoring data along the PN line (see Fig. 1 for its position) in the ECS.

3 Results

3.1 Temporal and spatial variations of chlorophyll-*a* and nutrients

For a direct comparison with the observations (Chen, 2009), we selected DIN as an example of simulated nutrients and presented its horizontal distribution in the surface and bottom layers for four seasons (Fig. 3). The corresponding observations can be found in Chen (2009).

In winter, the surface DIN concentration was high along the western coast of the ECS and eastern coast of the Yellow Sea, but was low in the central Yellow Sea and the northwestern coast of the Yellow Sea (Fig. 3a). The lowest DIN concentrations were found along and out of the shelf break where there is the occurrence of nutrient-poor Kuroshio surface water. Because of tidal mixing and strong wind stirring in winter months, the DIN in the bottom layer of the Yellow Sea and the inner shelf of ECS (Fig. 3b) displayed a similar distribution to that observed in the surface layer (Fig. 3a). However, in the bottom layer of the middle and outer shelves, the DIN concentration was higher than that of the surface layer. Apparently, the onshore transport of nutrient-rich Kuroshio subsurface water across the shelf break contributed to this distribution. High nutrients northeast of Taiwan and west of Kyushu in the bottom layer were consistent with the spatial distribution of Kuroshio onshore transport along the shelf break in the ECS (Guo et al., 2006).

In spring, surface DIN concentrations are similar to levels observed in winter along western coast of the ECS, but decreases sharply in the central Yellow Sea and from middle shelf to outer shelf of the ECS (Fig. 3c). In the bottom layer (Fig. 3d), the DIN concentration decreased markedly in the Taiwan Strait but increased from north Taiwan to the middle shelf south of 30° N; bottom DIN also increased in the central Yellow Sea. The decrease in surface nutrients is easily related to the intensification of biological activity and the reduction of nutrients supply from the lower layer to the upper layer in spring. With increasing of solar radiation and weakening of winds from winter to spring, stratification in the ECS and Yellow Sea has formed by May. Thermal stratification

reduces upward transportation of nutrients from the bottom layer to the surface layer. At the same time, the dissolved nutrients released by the remineralization of sinking particulate organic matter in the bottom layer were kept there, inducing an increase in DIN. In addition, the intensification of Kuroshio subsurface water intrusion in spring may also influence the increase of DIN in the bottom layer over the middle and outer shelves (Jacobs et al., 2000).

In summer, a significant change in the surface layer is the dispersal of nutrient-poor water (DIN<1 mmol m^{-3}) from the central area to coastal areas in the Yellow Sea, and the offshore spreading of nutrient-rich water (DIN>1 mmolm^{-3}) from the Changjiang estuary toward Jeju Island in the ECS (Fig. 3e). The reduction of surface nutrients in the Yellow Sea can be easily explained by the intensification of stratification in summer, while the mechanism of long distance offshore transport of nutrients from the Changjiang estuary has been given by Isobe and Matsuno (2008). In the bottom layer, nutrients increased in the northern shelf of the ECS (southwest of Jeju Island) but decreased in the offshore area of Changjiang estuary and the northern part of the Yellow Sea (Fig. 3e,f).

In autumn, the concentration of surface DIN was low in the central Yellow Sea and over the middle and outer shelves of the ECS, with increased levels in the western and eastern coasts of the Yellow Sea (Fig. 3g). In the bottom layer (Fig. 3h) nutrient-rich water was found from the central Yellow Sea to the northern shelf of the ECS, and farther to the shelf break, indicating a possible route of nutrient supply from Kuroshio subsurface water.

In general, not only nutrients but also light intensity, water temperature and stratification controlled phytoplankton growth in the surface water. With increasing surface temperatures in spring, the water column becomes stable and high surface chlorophyll-*a* initially appears in the central region of Yellow Sea during April (Fig. 4). From April to September, the high surface chlorophyll-*a* area moved gradually to coastal waters of the Yellow Sea. Meanwhile, a band of high surface chlorophyll-*a* was maintained from the western Yellow Sea to the offshore region of the Changjiang estuary. In autumn

(e.g., October) slightly higher chlorophyll-*a* values were found again in the central region of the Yellow Sea. In the area from the Changjiang estuary to the ECS shelf break, a high surface chlorophyll-*a* area appeared firstly at the outer shelf (northeast of Taiwan) in winter (e.g., January), then gradually moved to the inner shelf from spring to summer, and remained offshore of the Changjiang estuary in autumn (e.g., October). The Changjiang River provides not only nutrients but also suspended sediments to the ECS. The reason for relatively low chlorophyll-*a* levels in close proximity to the estuary is due to high turbidity caused by the amount of suspended sediments from the Changjiang River, significantly weakening subsurface light intensity.

3.2 Vertical distribution of chlorophyll-*a* and nutrients along a transect across the shelf break

There is an established transect in the ECS, called the PN line, where hydrographic surveys have continued for more than 40 years by JMA. Usually, the survey is carried out four times a year, with each survey corresponding to one season. Here we first describe the common features of nutrients and chlorophyll-*a* in the observations and model results (Figs. 5 and 6), then address the possible causes for the differences between the observations and model results. The observations are from nutrients (represented by DIN) and chlorophyll-*a* averaged in each season from 1965 to 2004, whereas the model results are the same variables but with monthly means from February, May, August and October, representing winter, spring, summer and autumn, respectively.

In winter, both nutrients and chlorophyll-*a* were vertically homogenous over the shelf due to intensive mixing. Nutrients were higher in the inshore side compared to the offshore side in the upper layer (water depth <100 m). The highest nutrients were found in the lower layer (water depth >100 m) from the shelf break to the open ocean, and are expected to be an important source of nutrients to the upper layer and middle shelf. Chlorophyll-*a* was high in the surface layer from the shelf break to the open ocean.

In spring, nutrients in the surface layer were quickly depleted with advent of phytoplankton growth. This occurred from the inshore side of the shelf to the shelf break, with the maximum chlorophyll-*a* occurring in the surface layer or shallow subsurface layer. With changes in phytoplankton production, the euphotic zone becomes shallower from the inshore side of the shelf to the shelf break, but becomes deep farther offshore. In the bottom layer, nutrient-rich water can be identified from the inshore side of the shelf to the shelf break. From the depth of the euphotic zone and distribution of nutrients, it can be deduced that the nutrient-rich bottom water largely contributes to phytoplankton growth.

In summer, the concentration of surface nutrients decreases and becomes a limiting factor on the growth of phytoplankton. With a decrease in surface phytoplankton, the euphotic zoon is deepened and phytoplankton can utilize nutrients in the deeper layer. Consequently, the subsurface chlorophyll-*a* maximum over the shelf appears deeper in summer than in spring and the concentration of nutrients in the bottom layer decreases slightly.

In autumn, the concentration of surface nutrients recovers slightly due to the intensification of surface mixing. Chlorophyll-*a* still has a large concentration in the middle layer, indicating a persistent contribution of nutrient-rich bottom water to primary production from spring to autumn.

Although we can confirm the above features from both observations and model results, differences were also apparent. For example, the high chlorophyll-*a* observed on the inshore side of the shelf in winter and autumn was not reproduced by the model. The high chlorophyll-*a* at the open ocean side was always found in model results but could not be confirmed in the model results. In addition, the concentration of chlorophyll-*a* in the subsurface layer over the shelf in summer and the concentration of nutrients below the subsurface layer from the shelf break to the open ocean side were generally higher in the model results than in the observations. These fundamental differences may have been caused by either incomplete observational data specified along the open boundary or incomplete structure of our biological module.

Improvement of the former depends on the extent of data collection east of Taiwan and within the Taiwan Strait, while the latter can be addressed by adding biological components such as zooplanktons, or by including additional processes such as microbial loop. Nevertheless, a continuous effort on improving the model performance is necessary in the future.

3.3 Seasonal and spatial variations in onshore fluxes of nutrients across the shelf break

Using flow velocity and nutrients concentration in the model results, we can calculate the onshore flux of water and nutrients across the shelf break of the ECS (Fig. 7), defined as the 200 m-isobath (Fig. 1) following Guo et al. (2006). Since it is the main stream of the Kuroshio that flows along the shelf break, flux across the shelf break in the ECS is also referred as the Kuroshio onshore flux. Because of this, our calculations can be compared to the nutrient flux from the Kuroshio water mass to the shelf of the ECS, previously estimated by Chen and Wang (1999) and Zhang et al. (2007b) who used a box model for the shelf of the ECS.

The volume of Kuroshio onshore flux displayed significant seasonal variation (Fig. 7), reaching a minimum of ∼0.5 Sv (1 Sv=10^6 m^3 s^{-1}) in June and a maximum of ∼3 Sv in November. The annual mean volume of Kuroshio onshore flux was estimated to be 1.53 Sv with a standard deviation of 0.97 Sv. All are consistent with the results calculated by a previous version of the hydrodynamic module (Guo et al., 2006), in which the tidal currents were excluded and river discharge was not explicitly included.

The Kuroshio onshore flux of DIN and DIP followed the seasonal variation in volume flux however there was a little difference. Both DIN and DIP reached a minimum in March, not in June when minimum volume flux occurs. Afterward, both increase gradually until November when they reached maximums of ∼16.0 kmol s^{-1} for DIN and ∼1.1 kmol s^{-1} for DIP; this was the same as the volume flux. The Kuroshio onshore flux of silicate showed different seasonal variation from those of volume, DIN and DIP. Silicate displayed a minimum in March as seen with DIN and DIP, however thereafter

it increased erratically. Before November when silicate reaches its maximum, we observed three peaks in the Kuroshio onshore flux of silicate.

The seasonal variations in Kuroshio onshore flux of DIN, DIP and silicate presented Fig. 7 is essentially consistent with those estimated by Zhang et al. (2007b) who showed a double input of DIN and DIP and a triple input of silicate from the Kuroshio to the shelf from summer to winter. The annual mean of Kuroshio onshore flux was 9.4 kmol s^{-1} for DIN, 0.7 kmol s^{-1} for DIP, and 18.2 kmol s^{-1} for silicate; the standard deviation was 4.6 kmol s^{-1} for DIN, 0.4 kmol s^{-1} for DIP, and 12.0 kmol s^{-1} for silicate. The annual means given here are at the same order as those estimated by the box models of 10.7 kmol s^{-1} for DIN, and 0.34 kmol s^{-1} for DIP from Chen and Wang (1999); 9.7 kmol s^{-1} for DIN, 0.65 kmol s^{-1} for DIP, 14.95 kmol s^{-1} for silicate from Zhang et al. (2007b).

In addition to quantifying total flux across the shelf break, the model results can also provide a spatial measure of the Kuroshio onshore flux of volume and nutrients along the shelf break (Fig. 8). There were two areas where positive onshore flux was concentrated. One was northeast of Taiwan where the Kuroshio bumps against the shelf break and induces a large onshore flux of water volume and nutrients. The integration of the Kuroshio onshore flux northeast of Taiwan (from point 1 to point 6 in Fig. 8) gave values of 5.8 Sv for volume, 21.1 kmol s^{-1} for DIN, 1.8 kmol s^{-1} for DIP and 48.3 kmol s^{-1} for silicate. The other was located southwest of Kyushu where the Kuroshio veers toward Tokara Strait and induces a large onshore flux of water volume and nutrients. The integration from this area (from point 22 to point 32 in Fig. 8) gave values of 0.5 Sv for volume, 7.8 kmol s^{-1} for DIN, 0.6 kmol s^{-1} for DIP and 18.7 kmols^{-1} for silicate. Along the shelf break between them, Kuroshio onshore flux of water volume and nutrients were generally negative, indicating an offshore transport of water and nutrients. Integration along the 200 m isobath from ∼26° N to ∼29° N (point 7 to point 21 in Fig. 8) gave values of −4.7 Sv for volume, −19.7 kmol s^{-1} for DIN, −1.6 kmol s^{-1} for DIP and −48.9 kmol s^{-1} for silicate.

4 Sensitivity experiments on the enrichment of oceanic nutrients

Although we obtained a positive onshore flux of oceanic nutrients across the shelf break, we still do not know whether these nutrients are involved in photosynthesis over the ECS shelf. As presented in Guo et al. (2006), half of the water through the Tsushima Strait is from the Kuroshio in summer and this ratio increases to 80% in winter. Therefore, it is possible that all the oceanic nutrients across the shelf break just flows toward the Tsushima Strait and maybe have no opportunity to contribute to the primary production over the ECS shelf.

Direct evaluation on how much the nutrients from the Kuroshio area contribute to the primary production over the ECS shelf needs to isolate the oceanic nutrients from the nutrients with other sources. This isolation is usually problematic in a nonlinear marine ecosystem. Instead of isolation, we applied sensitivity experiments, in which we artificially changed the nutrients concentration of the Kuroshio water specified along the lateral boundary of the model and consequently changed the supply of oceanic nutrients across the shelf break from the Kuroshio. The difference in the results between the sensitivity experiments and the simulation presented in Sect. 3 (hereafter referred as the control experiment) is caused only by the change in the supply of oceanic nutrients across the shelf break and therefore can give us some insight as to the role of oceanic nutrients in lower trophic level dynamics of the ECS ecosystem.

We carried out four sensitivity experiments, in which only the concentrations of nutrients (DIN, DIP and silicate) from sea surface to the bottom along the southern boundary (from Taiwan to 124° E) where Kuroshio water occupies were multiplied by a constant of 1.1, 1.2, 1.3 and 1.4. The other boundary conditions and initial conditions as well as model integration schedule were the same as those in the control experiment. As a result, the onshore flux of volume across shelf break was the same between the sensitivity experiments and the control experiment, with onshore flux of nutrients artificially increased in the sensitivity experiments.

4.1 Changes in surface nutrients and chlorophyll-*a* over the shelf of the ECS

The additional oceanic nutrients (e.g. DIN) in the surface layer appeared mostly offshore of the Changjiang estuary (Fig. 9). In summer (June–August), the positive anomaly of DIN concentration (sensitivity experiment – control experiment) was found along the coastal area from 29° N to 34° N, in which the offshore DIN anomaly was negative. After September, the area with a positive anomaly of DIN concentration was enlarged and extended to the Jeju Strait (the channel between Jeju Island and southern coast of Korea) and farther to the Tsushima Strait in winter (December–February). After March, the DIN positive anomaly gradually retreats to the coastal area. Although not as apparent as offshore the Changjiang estuary, the additional oceanic nutrients could also be identified over the middle and outer shelves in winter.

The response of chlorophyll-*a* in the surface layer to additional oceanic nutrients in winter appeared in the pathway of the Kuroshio, in particular northeast of Taiwan where a local maximum in the anomaly of chlorophyll-*a* between the sensitivity and control experiment can be identified (Fig. 10). The additional oceanic nutrients do not produce additional chlorophyll-*a* over the shelf in winter, which can be understood from the low chlorophyll-*a* levels over the shelf in the control experiment (Fig. 4). Apparently, primary production over the shelf in winter is not nutrient limited.

From May to September, the positive anomaly of chlorophyll-*a* in the surface layer caused by additional oceanic nutrients appeared in the offshore region of the Changjiang estuary. A part of the area with a positive anomaly of chlorophyll-*a* (Fig. 10) corresponded to the area with a negative anomaly of DIN in the inner shelf, offshore the Changjiang estuary (Fig. 9). This feature was caused by different ratios of DIN to DIP in the Changjiang River water and in the Kuroshio water and will be discussed in more detail in Sect. 4.3.

4.2 Changes in subsurface nutrients and chlorophyll-*a* across the shelf of the ECS

The increment of oceanic nutrients applied to the sensitivity experiments depended on the original concentration in the control experiment, and therefore was small in the surface layer and large in the subsurface and bottom layer. From January to March, the contours of additional oceanic DIN concentration were horizontally distributed along the PN section (Fig. 11), indicating a small supply of oceanic nutrients across the shelf break in winter. From April to June, the contours of 1 mmol m^{-3} and 2 mmol m^{-3} of additional DIN concentration moved from the shelf break to the middle and inner shelf (Fig. 11), suggesting the intrusion of Kuroshio subsurface water onto the bottom layer over the shelf. From July to October, the high concentration of additional oceanic DIN as represented by the contour of 2 mmol m^{-3} (Fig. 11) was maintained at the bottom layer over the shelf. This high concentration of additional oceanic DIN shows an onshore movement in November but retreats to the shelf break in December (Fig. 11). According to the fact that the supply of oceanic nutrients to the middle and inner shelves weakens in winter, the high concentration of additional oceanic nutrients offshore the Changjiang estuary from November to next April (Fig. 9) are those that have intruded in spring or summer.

The additional oceanic nutrients cause an increase in chlorophyll-*a* in the surface layer in cold months (November to next March) and in the subsurface in warm months (June to October) (Fig. 12). April and May appears to be a transition period when the increase in chlorophyll-*a* moves from the surface to subsurface layer. By observing shifts in euphotic depth in Fig. 11, we can infer the consumption of additional oceanic nutrients in the subsurface layer. Therefore, the stable concentration of additional oceanic DIN at the bottom layer over the shelf from June to October (Fig. 11) reflects a balance between consumption and supply of oceanic nutrients. With the same idea, an increase in additional oceanic DIN at the bottom layer over the shelf in November

(Fig. 11) can be caused by either a reduction in phytoplankton growth (Fig. 12) or an increased supply of oceanic nutrients, or both.

4.3 Changes in nutrients flux across the shelf break and the influence of element ratio of oceanic nutrients on the consumption of nutrients over the shelf

With an increase in the concentration of oceanic nutrients in the sensitivity experiments, the onshore flux of DIN, DIP and silicate across the 200 m-isobath generally increased in the same ratio (Table 1). This is a natural result since the onshore flux of volume does not change in all of these calculations. However, there is also an apparent difference in the increased ratio of three elements of nutrients. The increased ratio of silicate was highest, while that of DIN was lowest. Such differences are probably related to the different elemental ratio of nutrients in the water pre-existing over the shelf that was transported in an offshore direction across the shelf break, and in the oceanic water that was transported in an onshore direction.

The ratio of DIN to DIP in total onshore flux of nutrients in the control experiment was 13 (=9.36/0.72 in Table 1), which is less than the Redfield ratio of 16 used in the model calculation; the average ratio of DIN to silicate is ~0.5, which is also less than the ratio of 16:15 used in the model calculation; the average ratio of silicate to DIP was 25, which is higher than the ratio of 15 used in model the calculation. As shown in Fig. 11, the additional oceanic nutrients can reach the offshore area of the Changjiang estuary, where nutrient limitation has been reported to be DIP based on the observed atomic ratio of DIN, DIP and silicate (Liu et al., 2003). In our simulation, the average ratio of DIN to DIP in Changjiang River water was 59, the average ratio of DIN to silicate 0.35, and the average ratio of silicate to DIP was 166. Consequently, nutrient limitation in our simulation was also dependent on DIP for the Changjiang diluted water that spreads offshore the Changjiang estuary in summer. This is why we obtained a negative anomaly in that region for DIN, between the control experiment and sensitivity experiments (Fig. 9). Therefore, the supply of oceanic nutrients to the

shelf contributed to phytoplankton growth not only by themselves but also by their element ratio, because the low ratio of DIN to DIP in the Kuroshio water promotes the consumption of DIN in the pre-existing shelf water.

5 Conclusions

By combining a low trophic level ecosystem model with a hydrodynamic model, we were able to reproduce general features of spatial and temporal variations in nutrients and chlorophyll-*a* in the Yellow Sea and ECS. Horizontally, the area with high chlorophyll-*a* first appeared in the central Yellow Sea in spring, and then it moved toward coastal zones in summer; in the ECS, the area with high chlorophyll-*a* first appeard northeast of Taiwan, i.e., at the outer shelf and shelf break in winter, and then gradually moved toward the middle and inner shelves in summer and autumn. Vertically, high chlorophyll-*a* appeared in the surface in spring at the middle and outer shelves and in the subsurface in summer and autumn, corresponding to changes in light intensity and nutrients.

The onshore flux of volume and nutrients across the shelf break, calculated from model results, have noticeable seasonal variations. The flux of onshore volume reaches a minimum in June and a maximum in November, while the flux of nutrients reach a minimum in March and a maximum in November. The annual average onshore flux was estimated as 1.53 Sv for volume, 9.4 kmol s^{-1} for DIN, 0.7 kmol s^{-1} for DIP, and 18.2 kmol s^{-1} for silicate. Along the shelf break of the ECS, areas northeast of Taiwan and southwest of Kyushu supply onshore flux of volume and nutrients, whereas the middle shelf break between them provides offshore flux of volume and nutrients.

By artificially increasing the concentration of oceanic nutrients in the Kuroshio water, we confirmed the contribution of oceanic nutrients to primary production over the shelf of the ECS. The additional oceanic nutrients distributed into the bottom layer from the shelf break to the offshore region of the Changjiang estuary from spring to summer, and appeared in the surface layer mainly from autumn to winter. The contribution of oceanic

nutrients to primary production over the shelf can be found not only in the surface layer (mainly at the outer shelf and shelf break in winter and in the region outside the turbidity zone of the Changjiang estuary in summer) but also in the subsurface layer over the shelf from spring to autumn.

Since the ratio of three elements of nutrients in the Kuroshio water was different from that in the pre-existing shelf water, in particular from the Changjiang plume, the contribution of oceanic nutrients to photosynthesis over the shelf promoted the consumption of residual DIN in that area. In this sense, it can be concluded that the supply of oceanic nutrients to the shelf of the ECS contributes to phytoplankton growth not only in itself but also by its element ratio.

Acknowledgements. The authors thank Jing Zhang at East China Normal University for the discussions on model results, Todd Miller at Ehime University for his help on English correction. Liang Zhao was supported by the National Science Foundation of China (No. 40806001 and 40830854), National Basic Research Program of China (973 Program 2010CB428904) and Global COE Program from the Japanese Ministry of Education, Culture, Sports, Science and Technology. Xinyu Guo was supported by Global COE Program from the Japanese Ministry of Education, Culture, Sports, Science and Technology and JSPS KAKENHI (21310012).

References

Blumberg, A. F. and Mellor, G. L.: A description of a three dimensional coastal ocean circulation model, in: Three-Dimensional Coastal Ocean Models, Coastal and Estuarine Series, No. 4, edited by: Heaps, N., Am. Geophys. Union, 1–16, 1987.

Chen, C. T. A.: Chemical and physical fronts in the Bohai, Yellow and East China Seas, J. Mar. Syst., 78(3), 394–410, 2009.

Chen, C. T. A. and Wang, S. L.: Carbon, alkalinity and nutrient budgets on the East China Sea continental shelf, J. Geophys. Res., 104(C9), 20675–20686, 1999.

Chen, D. X.: Marine Atlas of Bohai Sea, Yellow Sea, East China Sea, Hydrology, edited by: Chen, G. Z., China Ocean Press, Beijing, 530 pp., 1992.

Dobson, F. W. and Smith, S. D.: Bulk models of solar radiation at sea, Q. J. Roy. Meteor. Soc., 114, 165–182, 1998.

Garcia, H. E., Locarnini, R. A., Boyer, T. P., and Antonov, J. I.: World Ocean Atlas 2005, Dissolved Oxygen, Apparent Oxygen Utilization, and Oxygen Saturation, vol. 3, edited by: Levitus, S., NOAA Atlas NESDIS 63, US Government Printing Office, Washington, DC, 342 pp., 2006.
Garcia, H. E., Locarnini, R. A., Boyer, T. P., and Antonov, J. I.: World Ocean Atlas 2005, Nutrients (phosphate, nitrate, silicate), vol. 4, edited by: Levitus, S., NOAA Atlas NESDIS 64, US Government Printing Office, Washington, DC, 396 pp., 2006.
Guo, X., Hukuda, H., Miyazawa, Y., and Yamagata, T.: A triply nested ocean model for simulating the Kuroshio-roles of horizontal resolution on JEBAR, J. Phys. Oceanogr., 33, 146–169, 2003.
Guo, X., Miyazawa, Y., and Yamagata, T.: The Kuroshio onshore intrusion along the shelf break of the East China Sea: the origin of the Tsushima Warm Current, J. Phys. Oceanogr., 36, 2205–2231, 2006.
Isobe, A.: Recent advances in ocean circulation research on the Yellow Sea and East China Sea shelves, J. Oceanogr., 64, 569–584, 2008.
Isobe, A. and Matsuno, T.: Long-distance nutrient-transport process in the Changjiang river plume on the East China Sea shelf in summer, J. Geophys. Res., 113, C04006, doi:10.1029/2007JC004248, 2008.
Jacobs, G. A., Hur, H. B., and Riedlinger, S. K.: Yellow and East China Seas response to winds and currents, J. Geophys. Res., 105, 21947–21968, 2000.
Kalnay, E., Kanamitsu, M., Kistler, R., and Collins, W.: The NCEP/NCAR 40-year reanalysis project, B. Am. Meteorol. Soc., 77(3), 437–471, 1996.
Liu, S. M., Zhang, J., Chen, H. T., Wu, Y., Xiong, Y., and Zhang, Z. F.: Nutrients in the Changjiang and its tributaries, Biogeochemistry, 62(1), 1–18, 2003.
Liu, S. M., Hong, G.-H., Zhang, J., Ye, X. W., and Jiang, X. L.: Nutrient budgets for large Chinese estuaries, Biogeosciences, 6, 2245–2263, doi:10.5194/bg-6-2245-2009, 2009.
Mellor, G. L.: Users guide for a three-dimensional, primitive equation, numerical ocean model, Program in Atmospheric and Oceanic Sciences, Princeton University, 53 pp., 2003.
Moll, A.: Regional distribution of primary production in the North Sea simulated by a three-dimensional model, J. Mar. Syst., 16(1–2), 151–170, 1998.
Skogen, M. D. and Søiland, H.: A User's guide to NORWECOM v2.0, in: The NORWegian Ecological Model system, Bergen, Institute of Marine Research, 42. Technical Report Fisken og Havet 18/98, 1998.

Skogen, M. D. and Moll, A.: Interannual variability of the North Sea primary production: comparison from two model studies, Cont. Shelf Res., 20(2), 129–151, 2000.
Wan, X. F., Wu, Z. F., Chang, Z. Q., and Zhang, X. L.: Reanalysis of atmospheric flux of nutrients to the South Yellow Sea and the East China Sea, Mar. Environ. Sci., 21(4), 14–18, 2002.
Wang, B. D., Wang, X. L., and Zhang, R.: Nutrient conditions in the Yellow Sea and the East China Sea, Estuarine, Coast. Shelf Sci., 58, 127–136, 2003.
Wang, Q., Guo, X. Y., and Takeoka, H.: Seasonal variations of the Yellow River plume in the Bohai Sea: a model study, J. Geophys. Res., 113, C08046, doi:10.1029/2007JC004555, 2008.
Wang, W. J. and Jiang, W. S.: Study on the Seasonal Variation of the Suspended Sediment Distribution and Transportation in the East China Seas Based on SeaWiFS Data, Journal of Ocean University of China (Oceanic and Coastal Sea Research), 7(4), 385–392, 2008.
Wang, Y. H.: Marine Atlas of Boshi Sea, Yellow Sea, East China Sea, Chemistry, edited by: Chen, G. Z., China Ocean Press, Beijing, 257 pp., 1991.
Wei, H., Sun, J., Moll, A., and Zhao, L.: Phytoplankton dynamics in the Bohai Sea-observations and modeling, J. Mar. Syst., 44, 233–251, 2004.
Zhang, G. S., Zhang, J., and Liu, S. M.: Characterization of nutrients in the atmospheric wet and dry deposition observed at the two monitoring sites over Yellow Sea and East China Sea, J. Atmos. Chem., 57, 41–57, 2007a.
Zhang, J., Liu, S. M., Ren, J. L., Wu, Y., and Zhang, G. L.: Nutrient gradients from the eutrophic Changjiang (Yangtze River) Estuary to the oligotrophic Kuroshio waters and re-evaluation of budgets for the East China Sea Shelf, Prog. Oceanogr., 74, 449–478, 2007b.
Zhang, J.: Nutrient elements in large Chinese estuaries, Cont. Shelf Res., 16(8), 1023–1045, 1996.

Table 1. Annual onshore fluxes of nutrients across 200 m isobath in control experiment and four sensitivity experiments. The positive flux is defined as onshore direction and the unit is kmol s^{-1}. "ctl" denotes control experiment while "+10%"–"+40%" denote the sensitivity experiments in which the concentration of oceanic nutrients in the Kuroshio water was artificially increased by 10%–40%, respectively. The values in brackets denote ratios of increased fluxes in sensitivity experiments to the initial flux in control experiment.

	ctl	+10%	+20%	+30%	+40%
DIN	9.4	10.4(+10.8%)	11.4(+21.5%)	12.3(+32.0%)	13.3(+42.3%)
DIP	0.72	0.80(+11.2%)	0.88(+22.3%)	0.96(+33.2%)	1.03(+44.1%)
SIL	18.2	20.4(+11.7%)	22.5(+23.3%)	24.6(+34.8%)	26.6(+46.2%)

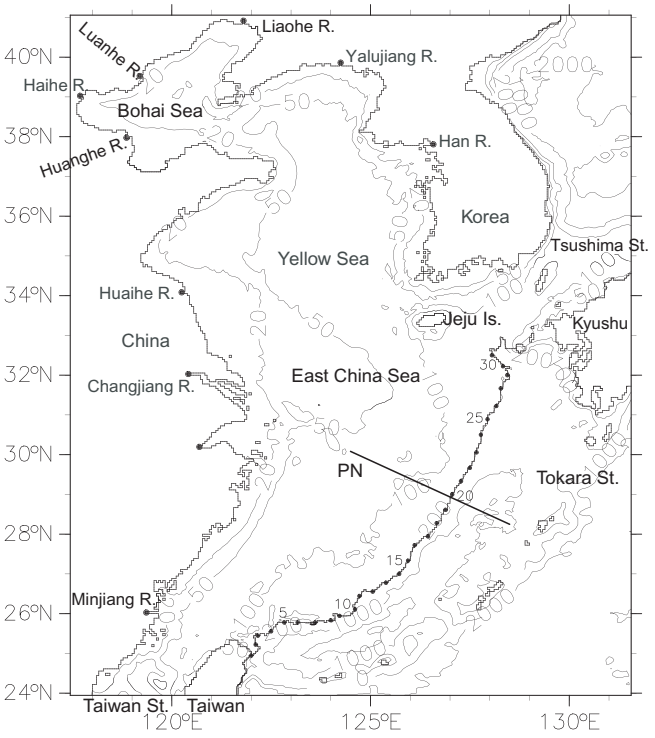

Fig. 1. Model domain and bathymetry. Contours with numbers are isobaths in meters. The 200 m-isobath along the shelf break is overlapped by a line with dots and numbers, across which the fluxes of volume and nutrients are calculated and presented in Figs. 7 and 8.

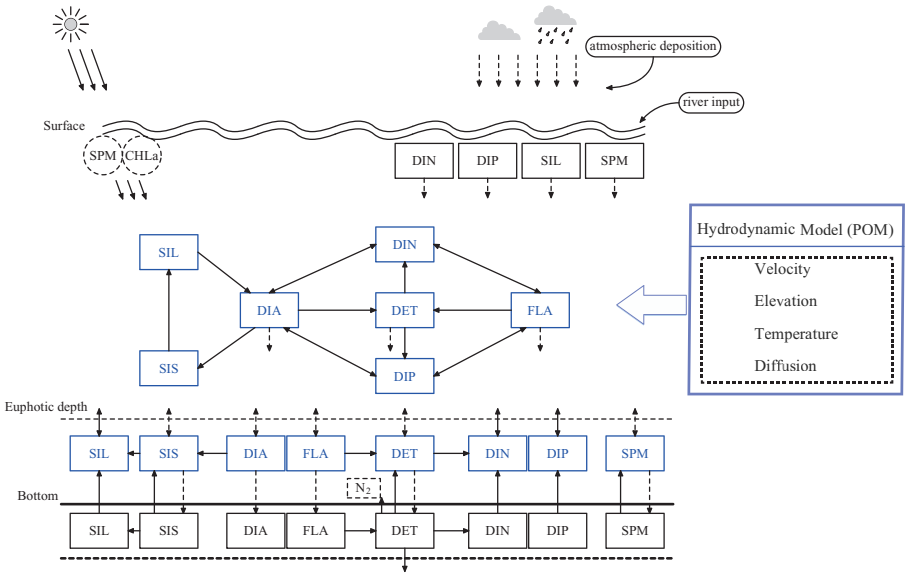

Fig. 2. Schematic illustration of the biophysical model. The hydrodynamic module is based on the Princeton Ocean Model (POM) (Mellor, 2003). The biological module includes three elements of nutrients (dissolved inorganic nitrogen, DIN; dissolved inorganic phosphorus, DIP; and silicate, SIL), two types of phytoplankton (diatoms, DIA; and flagellates, FLA), and two types of biogenic organic materials (dead organic matter, DET; and biogenic silica, SIS). Equations for the processes among these variables are from Skogen and Søiland (1998). The extinction coefficient of photosynthetic active radiation is affected by the concentrations of both suspended particulate matter (SPM) and chlorophyll-*a* (CHLa).

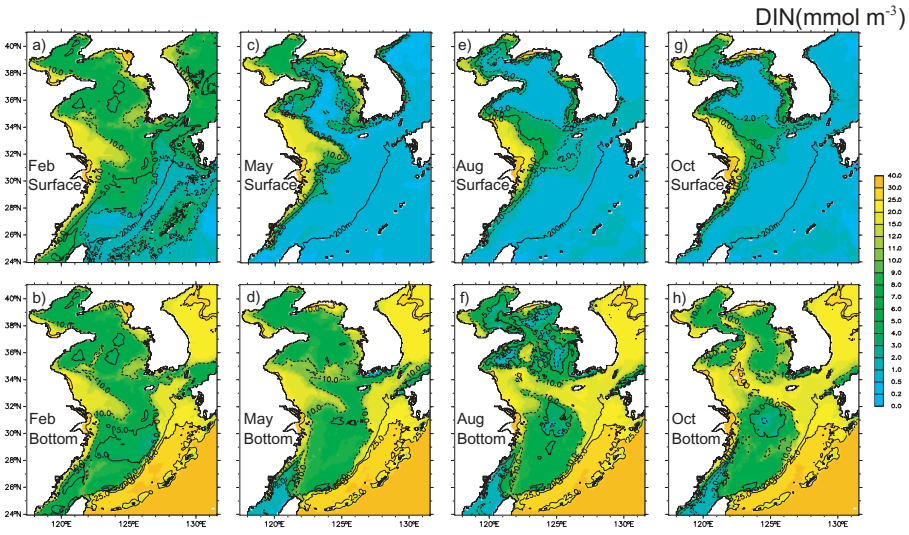

Fig. 3. Horizontal distribution of simulated DIN (mmol m^{-3}) at the surface (2 m depth) and bottom layer (the deepest sigma layer) in four seasons.

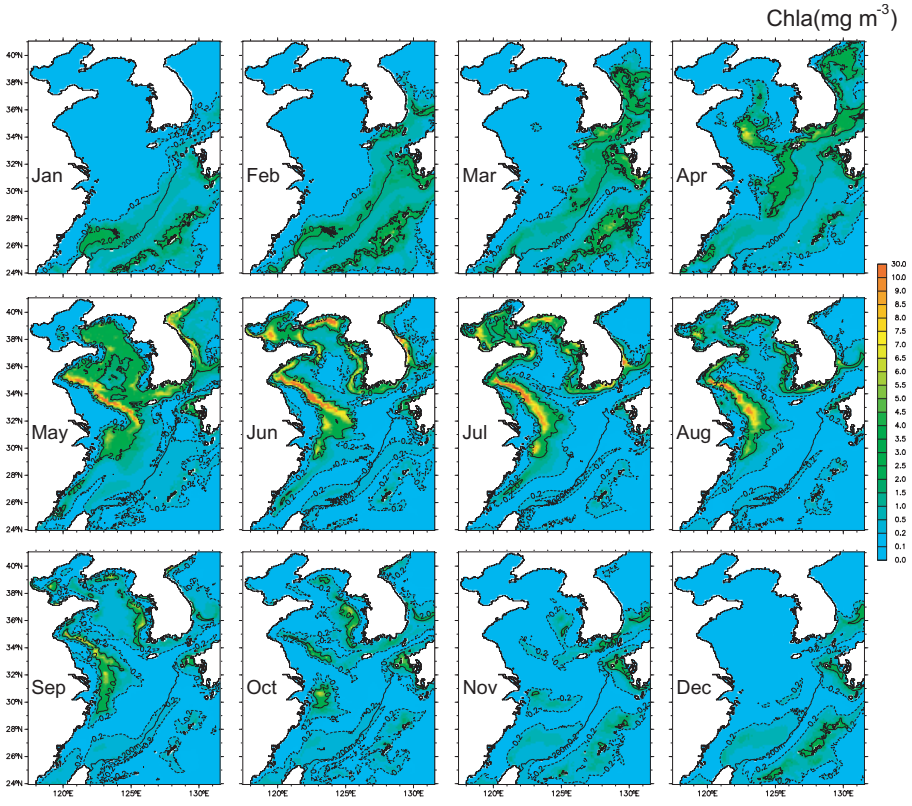

Fig. 4. Horizontal distribution of simulated chlorophyll-*a* (mg m^{-3}) at the surface layer (2 m depth) in 12 months.

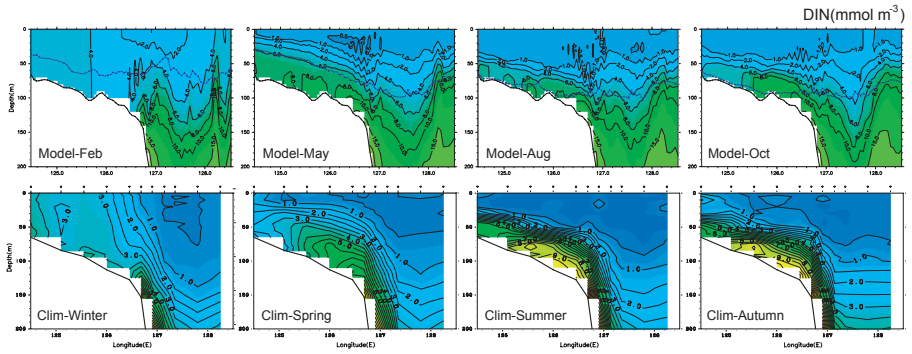

Fig. 5. Simulated (upper panels) and observed (lower panels) distributions of DIN (mmol m^{-3}) along the PN line in four seasons. Dashed blue line in the upper panels denotes euphotic depth.

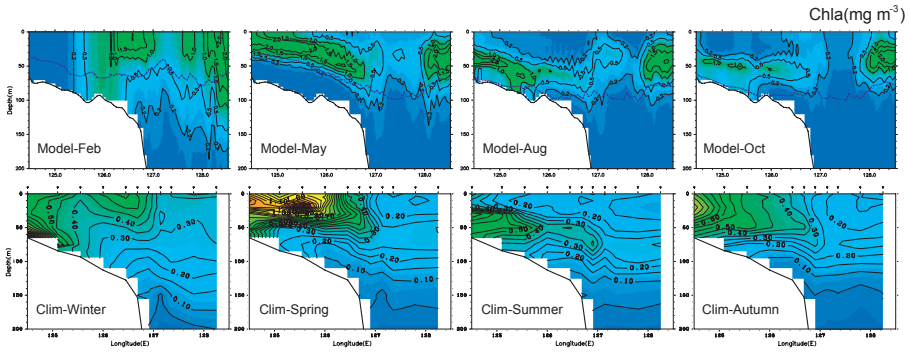

Fig. 6. The same as Fig. 5 but for chlorophyll-*a* (mg m^{-3}).

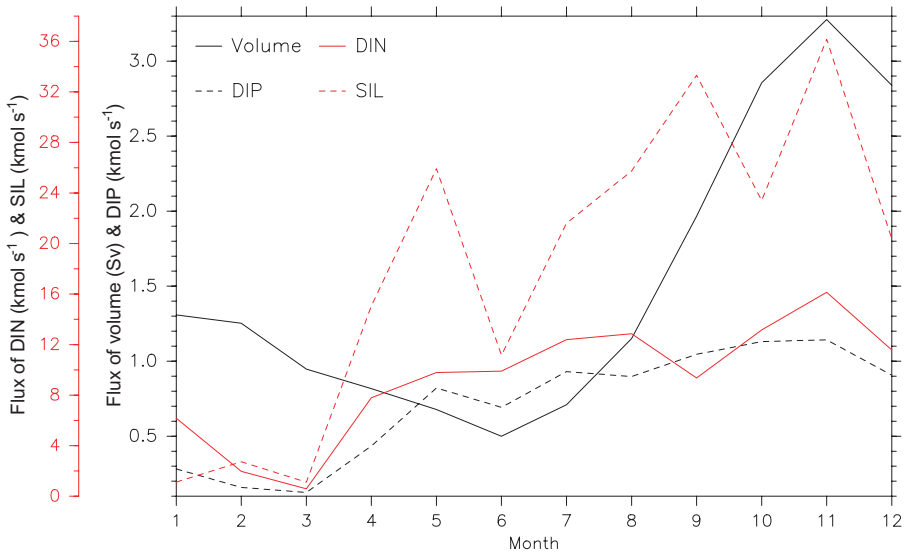

Fig. 7. Monthly onshore flux of volume (Sv) and nutrients (kmol s^{-1}) across the entire 200 m-isobath shown in Fig. 1. The positive direction of flux is toward the shelf of the ECS. Black solid line denotes volume, red solid line for DIN, black dashed line for DIP, and red dashed line for SIL.

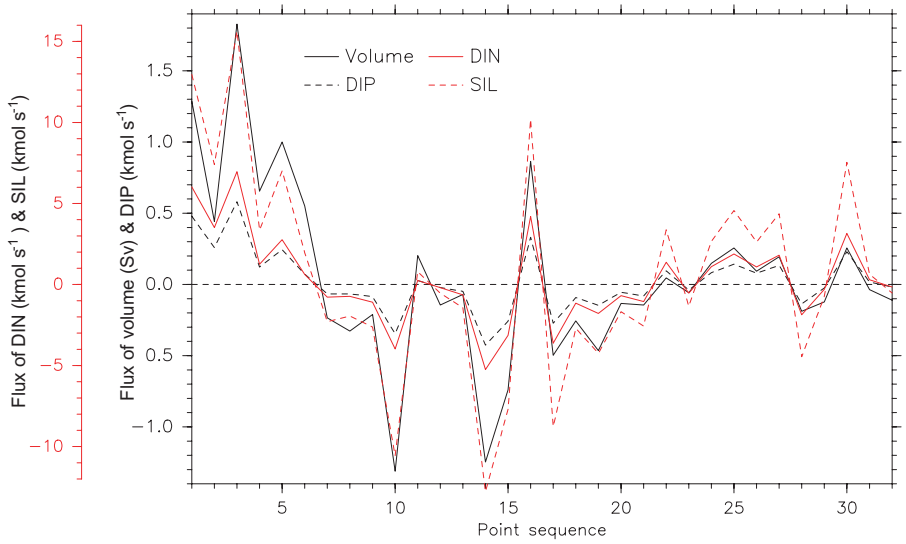

Fig. 8. Spatial distribution along the 200 m-isobath of annual averaged onshore flux of volume (Sv) and nutrients (kmol s^{-1}). The value at each point is the integrated flux between two points denoted by dots along the 200 m-isobath in Fig. 1. The positive direction is toward the shelf of the ECS. Black solid line denotes volume, red solid line for DIN, black dashed line for DIP, and red dashed line for SIL.

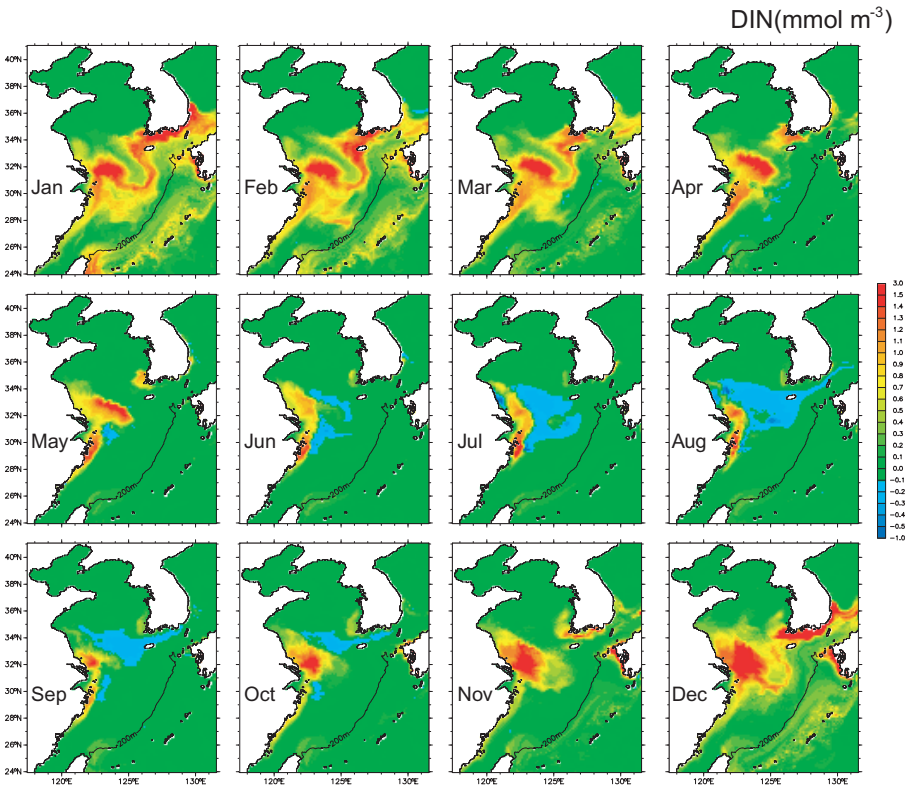

Fig. 9. The anomaly of monthly DIN (mmol m^{-3}) at the surface layer (2 m depth) between the sensitivity experiment, in which the oceanic nutrients were enriched by 30%, and the control experiment.

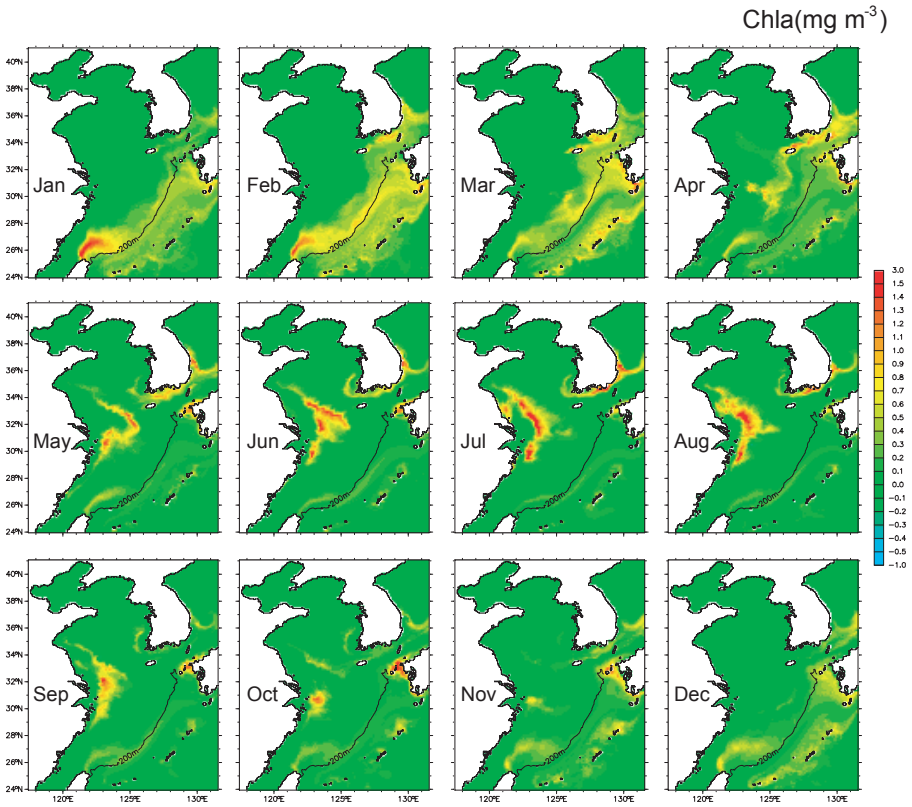

Fig. 10. The same as Fig. 9 but for chlorophyll-*a* (mg m^{-3}).

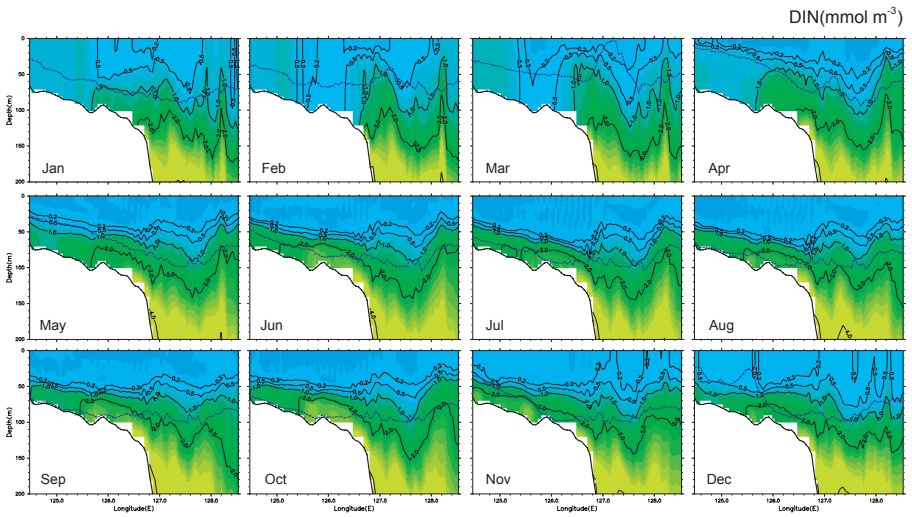

Fig. 11. The anomaly of monthly DIN (mmol m^{-3}) along the PN line between the sensitivity experiment, in which the oceanic nutrients are enriched by 30%, and the control experiment. Dashed blue line denotes euphotic depth.

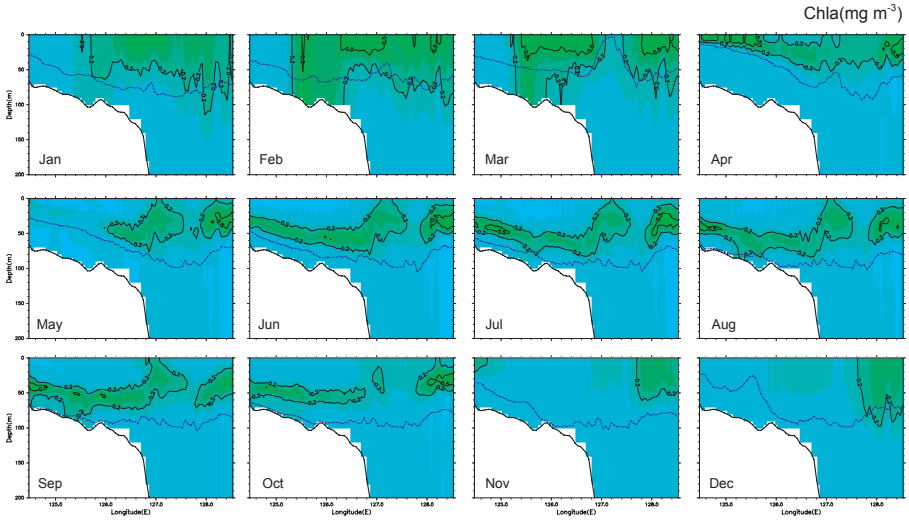

Fig. 12. The same as Fig. 11 but for chlorophyll-*a* (mg m^{-3}).